

## **INITIAL 1-D SINGLE PHASE LIQUID VERIFICATION OF CTF**

**Chris Dances and Dr. Maria Avramova**

Department of Mechanical and Nuclear Engineering  
The Pennsylvania State University  
137 Reber Building, University Park, PA, 16802, USA  
cad39@psu.edu; mna109@psu.edu

**Dr. Vince Mousseau**

Computer Science Research Institute  
Sandia National Laboratories  
1450 Innovation Parkway, Albuquerque, NM 87123, USA  
vamuoss@sandia.gov

### **ABSTRACT**

Nuclear engineering codes are being used to simulate more challenging problems and at higher fidelities than for which they were initially developed for. In order to expand the capabilities of these codes, state of the art numerical methods and software quality measures need to be implemented. One of the key players in this effort is the Consortium for Advanced Simulation of Light Water Reactors (CASL) through development of the Virtual Environment for Reactor Applications (VERA). The sub-channel thermal hydraulic code used in VERA, COBRA-TF (Coolant-Boiling in Rod Arrays - Three Fluids), is partially developed at the Pennsylvania State University by the Reactor Dynamics and Fuel Management Research Group (RDFMG). The RDFMG of version COBRA-TF is referred to as CTF.

In an effort to help meet the objectives of CASL, a version of CTF has been developed that solves the residual formulation of the one dimensional single-phase conservation equations. The formulation of the base equations as residuals allows for the isolation of different sources of error and is a good tool for verification purposes. This paper outlines the initial verification work of both the original version of CTF and its residual formulation. The verification problem is a simple 1-D single phase liquid channel with no heat conduction, friction, and gravity. A transient boundary condition is applied that alters the inlet density and temperature while keeping the velocity within the channel constant. The constant velocity simplifies the modified equation analysis and the order of accuracy is readily obtained. A Richardson extrapolation is performed on the problem on the temporal and spatial step sizes to determine the convergence and order of accuracy of the discretization error. While extensive validation work has been present for CTF, there has been little to no verification work previously.

*Key Words:* CTF, thermal hydraulic, verification, residual, Richardson extrapolation, CASL

## 1 INTRODUCTION

For the past several decades, the primary focus in nuclear engineering within the United States has been on light water reactors (LWR). Commercially, all nuclear reactors are either boiling water reactors (BWR) or pressurized water reactors (PWR). Correct computation of the thermal hydraulics within the reactor core leads to efficient design and accuracy in the safety analysis. A popular subchannel code for modelling the hydrodynamics within the reactor core is CTF, which is a subchannel thermal-hydraulics code developed from COBRA-TF [1]. This FORTRAN based code solves 8 conservation equations for liquid, entrained droplet, and vapor phases, plus one conservation equation for non-condensable gases. A 1-D residual formulation of the code has been created. While other residual formulations have been formed for other versions of CTF [2], none have been integrated into the CASL version of CTF. This paper outlines an initial verification of the original version of the code as well as the residual version of the code. The verification problem is a single phase 1-D channel with transient inlet density and mass flow rate. The problem will undergo a Richardson's extrapolation in the temporal and spatial domains to verify the convergence and order of accuracy of the error. The study of the order of accuracy is considered one of the more rigorous verification criteria [3].

## 2 CTF

The thermal hydraulics of a LWR core is an important part of nuclear reactor design. CTF solves 9 conservation equations for liquid, entrained droplet, non-condensable gases, and vapor phases of water boiling within the rod structure of a LWR reactor core. Currently, the conservation equations analytically reduce into a pressure matrix in a semi-implicit method with rod temperatures solved for explicitly. The residual formulation of the code currently solves the 1-D single phase liquid conservation equations and calculated variables in a residual formulation. While it has the ability to solve the conservation equations semi-implicitly or implicitly, only the semi-implicit solution method is considered in this paper. This residual formulation should allow for easier and more in depth verification analysis. This paper details the initial comparison of the residual formulation to the original code.

### 2.1 Software Quality Assurance

Software quality assurance is a set of tools and procedures that helps ensure that the software is reliable. CTF is managed by GitHub repository setup and maintained by CASL. An extensive test matrix is run before each major push to ensure that the code meets the specified requirements. The test matrix consists of unit tests, code coverage runs, validation problems, and challenge problems. The code documentation consists of a theory manual, a user manual, a developer manual, a validation manual, and a developers manual. This paper will be the beginning of a verification manual, integrating this verification problem directly into the test matrix.

## 2.2 1-D Single Phase Liquid Conservation Equations

The finite volume structure in CTF in figure 1 is for a one-dimensional channel in the axial direction with  $n$  number of cells. The first and last cells at 0 and  $n + 1$  are ghost cells and act as the boundary conditions for the problem. Pressure, enthalpy, and density are averaged over the cell volume and are located at the center of the cell. Mass flow rate and velocity are located at the faces in between cells. The cells are represented with an index  $i$ , and the faces with indexes of  $i + \frac{1}{2}$  or  $i - \frac{1}{2}$ . This project will initially focus on this 1-D configuration. Usually the code is 3-D, with channels connecting to each other in two more dimensions.

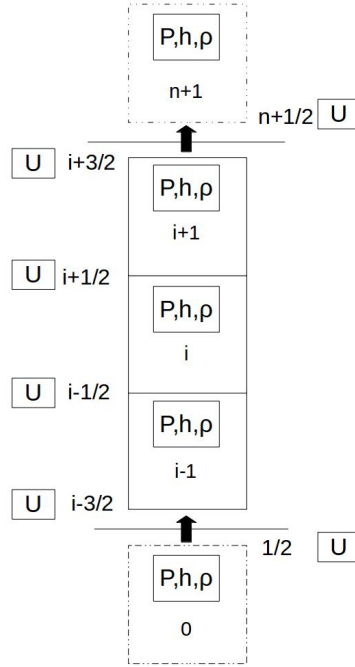


**Figure 1. The finite volume structure for CTF**

The single phase Euler partial differential equations for mass (1), momentum (2), and energy (3) correspond to the unknown variables pressure  $P$ , velocity  $u$ , and enthalpy  $h$ . Density  $\rho$  is related through an equation of state [4] as a function of enthalpy and pressure. For this work, the equation of state will be assumed to be approximately linear. This assumption should be valid due to the small changes in pressure and enthalpy observed during the verification problem.

$$\frac{\partial \rho}{\partial t} + \nabla \rho u = 0 \quad (1)$$

$$\frac{\partial \rho u}{\partial t} + \nabla \rho u^2 + \nabla P - \rho g = 0 \quad (2)$$

$$\frac{\partial \rho h}{\partial t} - \frac{\partial P}{\partial t} + \nabla(\rho u h) = 0 \quad (3)$$

### 2.3 Residual Formulation and Jacobian Construction

A residual is simply the difference between the value at some future iteration  $k + 1$  and the value at the current iteration  $k$ . Currently in CTF, the future iteration is taken to be the next time step  $n + 1$  and the current iteration is the current time  $n$ . The residual can be expressed for desired variables or conservation equations. For example, the residual for density,  $\delta \rho_i$ , is the difference between iterate levels  $k + 1$  and  $k$ ,  $\rho_i^{k+1} - \rho_i^k$ . The residuals for the equations are determined by substituting the residuals into the discretized equations, which should effectively change all  $n + 1$  into  $k$ . Each cell will have three residual variables and three residual equations. For the entire solution, we will then have a residual variable array  $\delta X$ , and a residual function array  $F(X)$  which defines a linear system  $J\delta X = -F(X)$ . The Jacobian matrix is defined as the derivative of each response of the function  $F_j$  with respect to each variable  $X_i$ . The derivative can be calculated numerically as shown by equation (4) where  $\epsilon$  is a small numerical value. Since the system is assumed to be linear, the approximation of the Jacobian matrix in this manner is also assumed to be accurate. As a check, the numerically computed Jacobian matrix was reduced to a pressure matrix using gaussian simulation and compared to the analytical pressure matrix from CTF. Each of the entries of the jacobian matrix appeared to match to nearly within machine precision.

$$J_{i,j} = \frac{\partial F_j(X)}{\partial X_i} \approx \frac{F_j(X_i + \epsilon) - F_j(X)}{\epsilon} \quad (4)$$

To build the Jacobian matrix, an object oriented class was created that contains three arrays. An array that points to the residual functions, an array that points to the position within a target variable array, and an array that has the index that the function is to be evaluated at. These lists can be appended in any order, but they have to be appended simultaneously such that variables and functions correspond with each other. To construct the Jacobian matrix, the residual function and residual variable arrays can each be looped over to numerically build the Jacobian matrix as seen in figure 2.

## 3 ISOKINETIC SINE WAVE ADVECTION

Code verification is the set of procedures set in place to ensure that the code was written properly. From least to most rigorous, the procedures are expert judgement, error quantification, consistency / convergence, and order of accuracy [5]. For this work, the Richardson Extrapolation will be used to check for convergence and order of accuracy of the error in space and time. The error should converge to zero, and the order of accuracy should converge to the values obtained through the modified equation analysis at the end of this section.

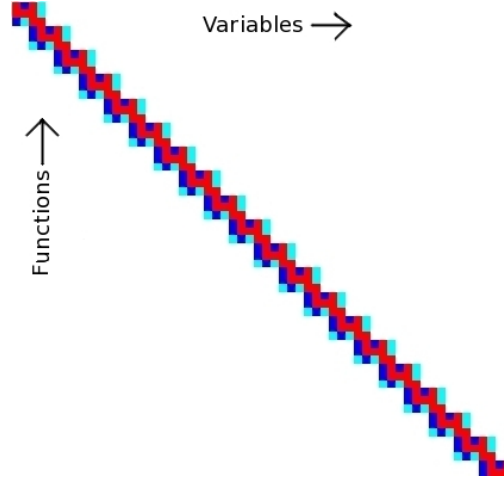


**Figure 2. Structure of the Jacobian matrix for single phase liquid**

### 3.1 Problem Setup

The verification problem is defined as a single horizontal channel with base parameters listed in table I. Channel area and perimeter are constant across the entire length of the channel. No grid spacers are present, and frictional losses are set to zero. Velocity and pressure are assumed to be constant, but small fluctuations may occur due to numerical roundoff. The channel geometry and operating conditions approximate a standard PWR. The inlet of the channel has a constant velocity with a fluctuating enthalpy that corresponds to a standard PWR rod bundle coolant channel.. The length of the transient was defined to be quadruple the time needed for the liquid at the inlet to advect to the outlet. The frequency of the sine wave was defined to generate a full period of a spatial wave across the length of the channel.

**Table I. Problem Parameters**

Parameter	Symbol	Value	Unit
Axial Length	$L$	3.6586	$m$
Channel Area	$A_{ch}$	4.94E-005	$m^2$
Wetted Perimeter	$P_w$	1.49E-002	$m$
Velocity	$V_o$	7.35	$\frac{m}{s}$
Pressure	$P_o$	155.00	bar
Temperature 1	$T_1$	290.00	$^{\circ}C$
Temperature 2	$T_2$	295.00	$^{\circ}C$
Enthalpy 1	$h_1$	1306.3	$\frac{kJ}{kg}$
Enthalpy 2	$h_2$	1310.9	$\frac{kJ}{kg}$
Mass Flow Rate 1	$\dot{m}_1$	0.2707	$\frac{kg}{s}$
Mass Flow Rate 2	$\dot{m}_2$	0.2672	$\frac{kg}{s}$
Final Time	$t_f$	2.00	sec
Wave Frequency	$\omega$	1.00	Hz

The lookup table to vary the inlet enthalpy  $h$  and inlet mass flow rate,  $\dot{m}$ , are generated from

equations 5 and 6 where  $x$  is the length from the inlet and  $t$  is the simulated time. The trigonometric functions assume constant axial spacing, time step size, and velocity. These equations should also behave as the known solutions throughout the entire domain of the problem. The enthalpy and mass flow rate vary proportionally to the density such that an isokinetic boundary condition is created at the inlet.

$$h(x, t) = \frac{1}{2} \left( (h_1 + h_2) + (h_1 - h_2) \cos \left( \omega \left( t - \frac{x}{V_o} \right) \right) \right) \quad (5)$$

$$\dot{m}(x, t) = \frac{1}{2} \left( (\dot{m}_1 + \dot{m}_2) + (\dot{m}_1 - \dot{m}_2) \cos \left( \omega \left( t - \frac{x}{V_o} \right) \right) \right) \quad (6)$$

The comparison between the data table and the output in CTF are shown for enthalpy and mass flow rate in figures 3 and 4, respectively. The CTF output was read from the high precision VTK data files at each point in time, which omitted the actual ghost cell where these values were applied. The CTF values are located at the nearest node to the inlet, and will experience small amounts of numerical diffusion. For large mesh sizes, this discrepancy is negligible as can be seen by the overlapping profiles in figures 3 and 4.

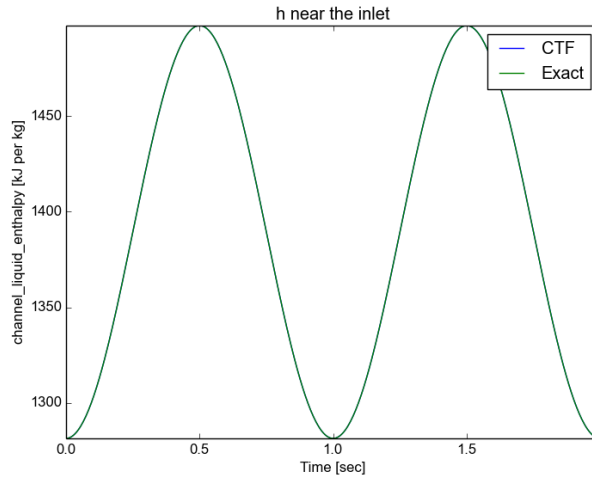


**Figure 3. Enthalpy Near the Inlet and the Analytical Solution**

The pressure and the velocity fluctuate by less than 0.5% during the simulation due to approximating the EOS as a linear function. This is considered small for this problem and should not greatly affect the order of accuracy of the error. The VTK output files allow for a high level of precision, reducing round off error in the output during the post processing.

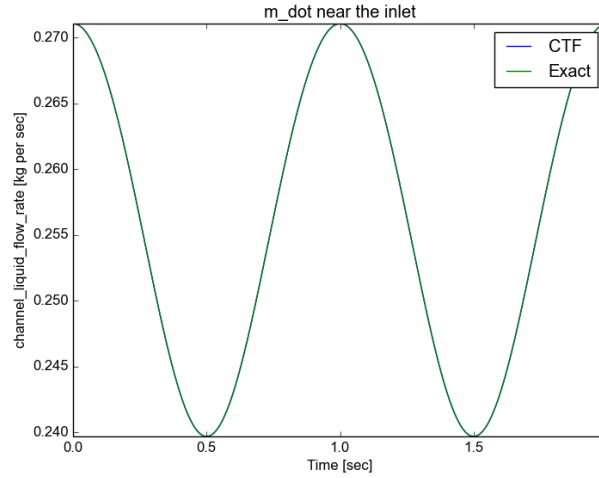


**Figure 4. Density Near the Inlet and the Analytical Solution**

### 3.2 Code Convergence

The current version of CTF uses global code convergence criteria that are used to estimate the rate of change of global mass and energy conservation. The transient values of these criteria are shown in figure 5 for the original version of CTF simulating the verification problem. Mass balance and storage are in units of  $\frac{kg}{s}$ . The energy balance, fluid energy, and solid energy are in units of  $kW$ . The solid energy storage is zero since there are not any heat structures present. The fluctuating values represent differences between the energy and mass entering and leaving the system. The flat profile for the mass storage term means that the sine wave has fully developed spatially through the channel.

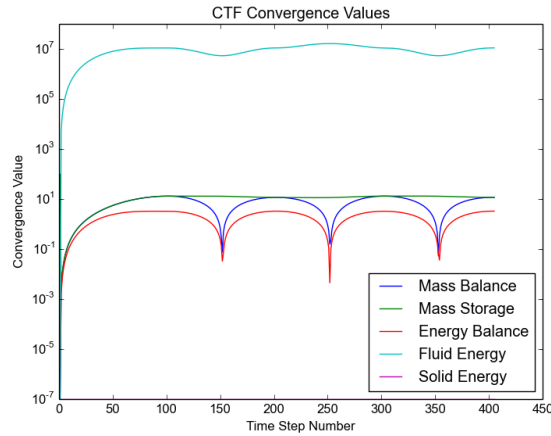


**Figure 5. Code Convergence Criteria for the Original Version of CTF**

The residual formulation prints out the summation of the equation residuals across the domain to an output file at the end of each time step and can be seen in figure 6. The mass equation residual is in units of  $\frac{kg}{m^3 s}$ . The energy equation residual is in units of  $\frac{kW}{m^3}$ . The momentum residual is in

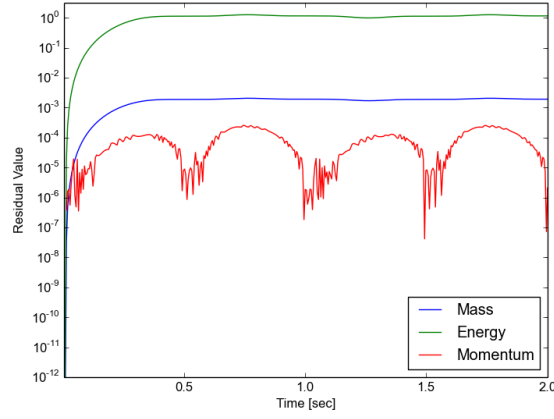


**Figure 6. Summation of the Residuals for the Residual Version of CTF**

units of  $\frac{kg}{m^2s^2}$ . The flat profile of the mass and energy residuals shows that the sine wave has fully developed spatially through the channel.

### 3.3 Modified Equation Analysis

The order of accuracy in time and space can be analytically determined for this problem through a modified equation analysis. Because the velocity is constant, it can be pulled out of the spatial derivative as shown in equation 7. Using upwinding, the finite difference can be written to look like equation 8. A second order Taylor series approximation can be used for  $\rho_i^{n+1}$  and  $\rho_{i-1}^n$  as shown in equations 9 and 10 respectively. The higher order terms ( $O(\Delta x^2, \Delta t^2)$ ) are not taken into account for this approximation. The Taylor series approximations can then be substituted into 8 to yield 11. This is the beginning of the modified equation analysis. The goal will be to isolate the original PDE and define the truncation error.

$$\frac{\partial \rho}{\partial t} + U_0 \frac{\partial \rho}{\partial x} = 0 \quad (7)$$

$$\frac{\rho_i^{n+1} - \rho_i^n}{\Delta t} + U_0 \frac{\rho_i^n - \rho_{i-1}^n}{\Delta x} = 0 \quad (8)$$

$$\rho_i^{n+1} = \rho_i^n + \frac{\partial \rho}{\partial t} \Delta t + \frac{1}{2} \frac{\partial^2 \rho}{\partial t^2} \Delta t^2 + O(\Delta t^3) \quad (9)$$

$$\rho_{i-1}^n = \rho_i^n - \frac{\partial \rho}{\partial x} \Delta x + \frac{1}{2} \frac{\partial^2 \rho}{\partial x^2} \Delta x^2 + O(\Delta x^3) \quad (10)$$



The lengthy equation 11 can be reduced to equation 12 since the  $\rho_i^n$  terms subtract out and the  $\Delta t$  and  $\Delta x$  terms in the denominator cancel out. This reduced equation can be re-written into equation 13, with the original PDE followed by the truncation terms.

$$\frac{\left(\rho_i^n + \frac{\partial \rho}{\partial t} \Delta t + \frac{1}{2} \frac{\partial^2 \rho}{\partial t^2} \Delta t^2\right) - \rho_i^n}{\Delta t} + U_0 \frac{\rho_i^n - \left(\rho_i^n - \frac{\partial \rho}{\partial x} \Delta x + \frac{1}{2} \frac{\partial^2 \rho}{\partial x^2} \Delta x^2\right)}{\Delta x} + O(\Delta x^2, \Delta t^2) = 0 \quad (11)$$

$$\frac{\partial \rho}{\partial t} + \frac{1}{2} \frac{\partial^2 \rho}{\partial t^2} \Delta t + U_0 \left( \frac{\partial \rho}{\partial x} - \frac{1}{2} \frac{\partial^2 \rho}{\partial x^2} \Delta x \right) + O(\Delta x^2, \Delta t^2) = 0 \quad (12)$$

The terms to the right of the original PDE are the first order accurate truncation terms. Notice how the truncation error is dependent on both the on the second derivatives of density with respect to space and time, and on the numerical spacing  $\Delta t$  and  $\Delta x$ . Since the truncation error is linearly dependent on  $\Delta t$  and  $\Delta x$ , the order of accuracy is 1 with respect to time and space.

$$\frac{\partial \rho}{\partial t} + U_0 \frac{\partial \rho}{\partial x} + \frac{1}{2} \frac{\partial^2 \rho}{\partial t^2} \Delta t - U_0 \frac{1}{2} \frac{\partial^2 \rho}{\partial x^2} \Delta x + O(\Delta x^2, \Delta t^2) = 0 \quad (13)$$

When the energy equation undergoes a similar modified equation analysis, the order of accuracy is also 1 for time and space. The momentum conservation equation does not apply for this problem since the velocity is constant.

## 4 RICHARDSON EXTRAPOLATION

The Richardson extrapolation was performed by refining the spatial and temporal step sizes by a factor of 2 for a set number of times. The spatial and temporal studies are refined separately in their own study in order to isolate the spatial and temporal affects on the solution. The generation of the inputs, running of the codes, and analysis of the output were automated with a python script in order to reduce user input errors and increase repeatability. The computational resources for the spatial study was much higher than the temporal study due to the need to keep the courant number below 0.500. To keep the computational resources needed to perform this analysis reasonable, fewer spatial refinements were performed compared to the temporal analysis.

### 4.1 Convergence of Error

The difference between iterations was computed at each time step and spatial location for each quantity of interest. This difference is considered as the error between each iteration. For the spatial refinement, the lower iterate values were numerically integrated to match the shape of the initial domain. The errors were then summed over the entire domain to yield a total error for each variable. The total error for density is plotted in figures 7 and 8 as a function of temporal and spatial step size.

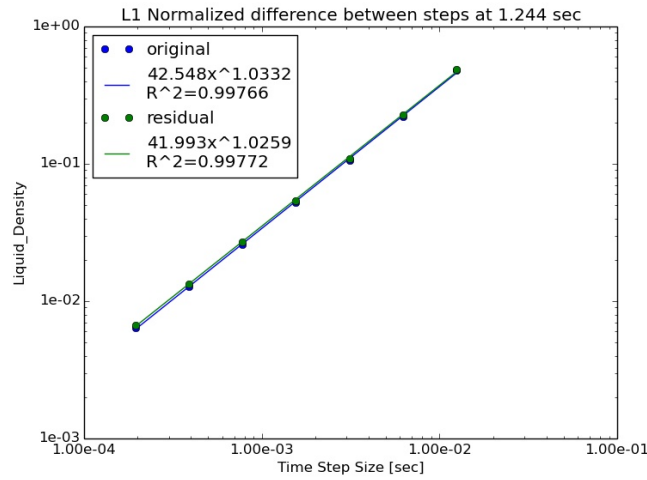


**Figure 7. Difference Between Successive Temporal Refinements for Density**

The data points were chosen to be inside of the asymptotic range as shown by the good power fit with an exponent near 1. The power fit shows that as the temporal and spatial step sizes are reduced, the numerical error approaches zero. The residual formulation and original versions of CTF show good agreement with each other.

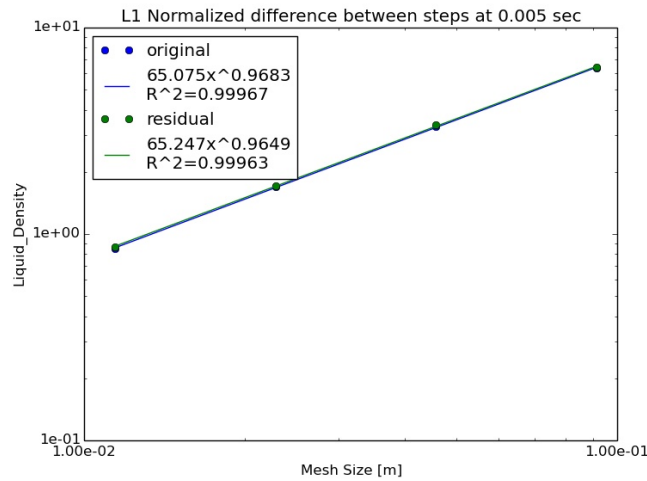


**Figure 8. Difference Between Successive Spatial Refinements for Density**

## 4.2 Order of Accuracy

The order of accuracy for this verification problem is first order as shown by the modified equation analysis. This can be considered to be the exponent on the power fits as seen in figures 7. However the order of accuracy  $p$  can be calculated by using equation 14 where  $f_1, f_2, f_3$  are consecutive levels within the same Richardson extrapolation study. The refinement factor,  $R$ , has the constant value of 2 for both the spatial and temporal studies.

$$p = \frac{\ln\left(\frac{f_3 - f_2}{f_2 - f_1}\right)}{\ln(R)} \quad (14)$$

The order of accuracy for all of the variables are presented for the temporal analysis and spatial analysis in figures 9 and 10 respectively. The temporal order of accuracy is well within the asymptotic range for the whole analysis, and moves closer to 1.0 with decreasing time step size. The spatial order of accuracy is a slightly outside the asymptotic range, but approaches an order of accuracy of 1.0 with decreasing mesh size.

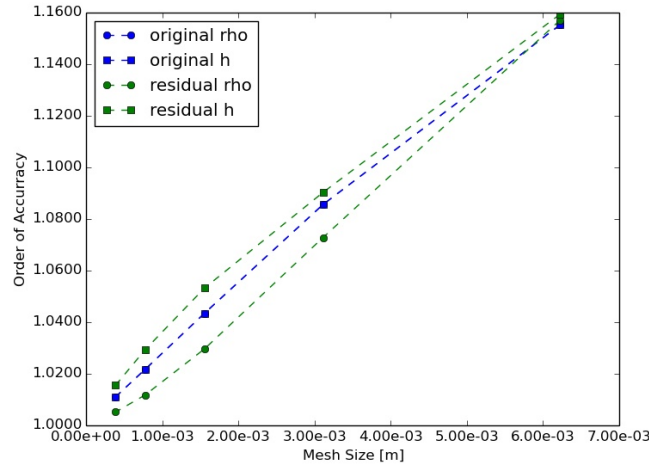


**Figure 9. Temporal Order of Accuracy**

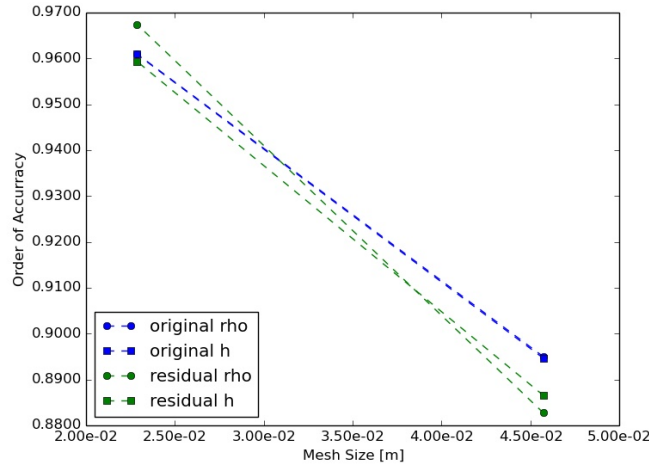


**Figure 10. Spatial Order of Accuracy**

The slight differences between the original version of CTF and the residual formulation might be due to the different solution methods and back substitution of variables. Despite the small

differences, both versions of the code exhibit order of accuracies very close the values obtained through the modified equation analysis.

## 5 CONCLUSIONS

The residual formulation of CTF allows for a numerical computation of the multivariable Jacobian matrix compared to the original analytical derivation of a pressure matrix. The 1-D isokinetic single phase liquid verification problem is a good verification problem through its isolation of the order of accuracies through modified equation analysis. The discretization error for both versions of the code converged to zero with decreasing time step and axial mesh size. The order of accuracy for the temporal and spatial refinements matched very closely with the modified equation analysis for both codes. For all of these data points, the residual formulation of the code showed discretization errors that were very close with the original version of the code. Future work might be comparing the numerical error obtained in the code to the analytical error predicted by the modified equation analysis using the derivatives of the known solutions. While within the asymptotic range, the first order accurate analytical error should almost exactly match the error from the code.

## 6 ACKNOWLEDGMENTS

Through CASL, this research used resources at the Oak Ridge National Laboratory and Sandia National Laboratories.

## 7 REFERENCES

- [1] R. K. Salko, “CTF Theory Manual,” (2014).
- [2] L. J. Lloyd, “Development of a Spatially-Selective, Nonlinear Refinement Algorithm for Thermal-Hydraulic Safety Analysis,” (2014).
- [3] C. J. Roy, “Review of code and solution verification procedures for computational simulation,” *Journal of Computational Physics*, **205**, pp. 131–156 (2005).
- [4] J. R. Cooper and R. B. Dooley, “The International Association for the Properties of Water and Steam Revised Release on the IAPWS Industrial Formulation 1997 for the Thermodynamic Properties of Water and Steam,” (2007).
- [5] W. L. Oberkampf and T. G. Trucano, “Verification and validation benchmarks,” *Nuclear Engineering and Design*, **238**, pp. 716–743 (2008).